

# Validate on Sim, Detect on Real – Model Selection for Domain Randomization

Gal Leibovich<sup>\*1</sup>, Guy Jacob<sup>\*1</sup>, Shadi Endrawis<sup>1</sup>, Gal Novik<sup>1</sup>, Aviv Tamar<sup>2</sup>

<sup>1</sup> Intel Labs

<sup>2</sup> Technion – Israel Institute of Technology

**Abstract**—A practical approach to learning robot skills, often termed *sim2real*, is to train control policies in simulation and then deploy them on a real robot. Popular techniques to improve the *sim2real* transfer build on domain randomization (DR) – training the policy on a diverse set of randomly generated domains with the hope of better generalization to the real world. Due to the large number of hyper-parameters in both the policy learning and DR algorithms, one often ends up with a large number of trained models, where choosing the best model among them demands costly evaluation on the real robot. In this work we ask – *can we rank the policies without running them in the real world?* Our main idea is that a predefined set of real world data can be used to evaluate all policies, using out-of-distribution detection (OOD) techniques. In a sense, this approach can be seen as a ‘unit test’ to evaluate policies before any real world execution. However, we find that by itself, the OOD score can be inaccurate and very sensitive to the particular OOD method. Our main contribution is a simple-yet-effective policy score that combines OOD with an evaluation in simulation. We show that our score – VSDR – can significantly improve the accuracy of policy ranking without requiring additional real world data. We evaluate the effectiveness of VSDR on *sim2real* transfer in a robotic grasping task with image inputs. We extensively evaluate different DR parameters and OOD methods, and show that VSDR improves policy selection across the board. More importantly, our method achieves significantly better ranking, and uses significantly less data compared to baselines.

## I. INTRODUCTION

Reinforcement learning (RL) is a popular method for learning various robotic skills [1]. Training and evaluating RL policies on a real robot, however, can be expensive, unsafe, and time consuming, and many recent RL advances were achieved by training policies in simulation and then transferring them to the real environment [2], [3], [4], [5]. Simulation allows straightforward parallelization during training, and modern physical simulators can quickly and safely simulate realistic physical interactions [6], [7].

Since simulation and reality often cannot be perfectly matched, policies trained in simulation do not necessarily perform well in the real world – a.k.a. the *sim-to-real* gap [8]. Several techniques have been proposed to alleviate the gap [9], and one of the most popular ones is *Domain Randomization (DR)* [10], [4], [11], where instead of training on a single simulation environment, models are trained on multiple domains with random variations in environment attributes such as textures, lighting, and dynamics. The hope

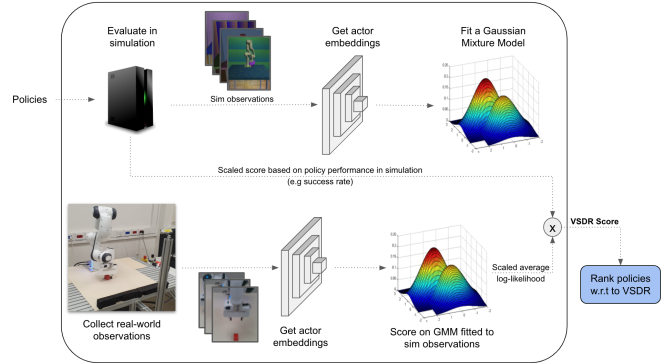


Fig. 1: We present an approach for selecting the best models to deploy in the real-world, by combining prior evaluation in simulation with out-of-distribution detection in the real world. Our method outperforms the compared baselines while requiring merely dozens of real-world observations. The bottom-left image in the diagram shows the lab setup used for real-world experiments, consisting of a Franka Panda robotic arm and an Intel RealSense D415 camera.

is that policies trained using DR will be invariant to these variations, and will therefore mitigate the *sim2real* gap.

Successfully running RL and DR algorithms often involves tuning a large number of hyper-parameters [12]. Selecting the best hyper-parameters with respect to performance in simulation is easy, and can even be done automatically using cross validation techniques [13]. However, how can we select the best parameters with respect to *real world* performance? This is the question we explore in this work. In particular, we seek to rank a set of models based on their real world performance. A naive solution is to run each model in the real world enough times to obtain an accurate performance evaluation. When the number of models is large, this approach can be very time consuming. For example, the manipulation task in our experiments requires 60-75 minutes of robot interaction to evaluate a single policy, and it is not uncommon to have hundreds of trained models when using deep RL algorithms.

We posit that a *fast cycle of model evaluation*, which does not require running the policies on the real robot, is critical for practical applications of *sim2real* methods. Specifically our desiderata from the evaluation method are:

- 1) Require only easy-to-obtain real world data.

<sup>\*</sup>Equal contribution

- 2) Accurate ranking of policies based on their real world performance.
- 3) Generally applicable to a wide range of robotic tasks.

To satisfy these requirements, we propose a simple-yet-practical approach that is composed of two components. The first component is out-of-distribution detection (OOD): we collect a set of real world observations that is independent of the trained policies, and evaluate whether this set is out-of-distribution with respect to the observations generated by DR and were used to train the policy. The idea is that if the DR robustness hypothesis indeed holds, then the real world should be seen as just another training environment, and therefore will not be identified as OOD. We find that a simple OOD method based on fitting a Gaussian mixture model (GMM) to the neural network activations already performs better than baselines based on offline policy evaluation [14]. However, the performance can be sensitive to the particular choice of OOD parameters. Our second component is an evaluation in simulation of the learned policies on held out DR environment attributes, in the spirit of a validation set; ideally, a well trained DR policy will obtain high performance on this evaluation. Our method combines both components into a single score, and we therefore term it *Validate on Sim, Detect on Real* (VSDR). Interestingly, we find that both components are complementary – the combined score improves on each individual component, in an extensive study of diverse parameter settings. More importantly, we show that VSDR can provide accurate and stable policy rankings.

To evaluate our method, we perform an extensive study on a robotic manipulation task with image inputs. We train over 60 models, using various RL and DR configurations, and collect over 130 hours of real-world evaluations. We then show that for various OOD methods and performance evaluation measures, VSDR consistently outperforms various baselines. We further evaluate the effect of model variability on ranking accuracy, and compare several protocols for collecting validation sets of real-world observations and their effect on model ranking.

## II. RELATED WORK

Recent studies of offline RL proposed metrics to evaluate a policy based on data collected from running a different policy. Most of these studies do not consider the sim-to-real gap, and assume that only the policy differs between train and test [15], [16], [17], [18], [19]. The closest work to ours is Off-Policy Classification (OPC [14]), which builds on actor-critic RL methods, and measures how accurately the trained critic classifies between successful or unsuccessful real trajectories. This method requires large amounts of very specific real-world data (successful vs. unsuccessful runs). In our experiments, even when such data was given, we found that our method significantly outperformed OPC.

Out-of-distribution detection, a.k.a. novelty detection or outlier detection, has been investigated extensively. Classical methods include one-class SVMs [20] and support vector data description [21], and more recent methods build on deep

generative models [22], [23]. Recently, for image domains, several methods proposed to first train a deep network on some image classification task, and then learn a probability distribution of the feature activation in the network, as displayed in the training data. In [24], a Gaussian distribution was used, while [25] extended this approach to flow-based distribution models. Here, we follow a similar approach, and learn the distribution of feature activations of the trained policy *when run on training environments*. We focus on GMMs, which we found to work well, but our approach can be used with other models, such as the ones in [24], [25].

## III. BACKGROUND

### A. Reinforcement Learning

We follow the Markov Decision Process (MDP) formulation of RL [26]. Consider an agent that at every time step  $t$  is in state  $s_t \in \mathcal{S}$ , executes an action  $a_t$  out of a set of possible actions  $\mathcal{A}$ , and transitions to a new state based on the transition probability  $s_{t+1} \sim p(s_{t+1}|s_t, a_t)$ . We denote the initial state distribution by  $P_{init}(s)$ . The agent also receives a reward  $r_t = R(s_t, a_t)$ . The goal is to find a policy  $a_t = \pi(s_t)$  that maximizes expected cumulative reward,  $\mathbb{E} \left[ \sum_{t=1}^T \gamma^t r_t \right]$ , where  $\gamma \in (0, 1]$  is the discount factor. The value of a state-action pair when following a policy  $\pi$ ,  $Q^\pi(s, a)$ , is defined as the expected sum of discounted rewards from that state-action pair:

$$Q^\pi(s, a) = \mathbb{E}_{a \sim \pi} \left[ \sum_{k=t+1}^{\infty} \gamma^{k-t-1} r_k \middle| s_t = s, a_t = a \right].$$

Actor-critic algorithms aim to find the optimal policy  $\pi^*(s_t)$  by using two functions approximators, one for the policy  $\pi_\theta(s_t)$  (actor) and the other for state-action value function  $Q_\phi^\pi(s_t, a_t)$  (critic). Specifically, we use *Soft Actor-Critic* (SAC) [27], [28] for our robot learning experiments.

### B. Sim2Real Transfer

Domain Randomization [10], [9], [29], [30] is a method for training neural network decision policies in simulation, such that their performance will transfer well to the real world. The idea is to apply random variations of the environment during the RL training. If these variations resemble the difference between simulation and reality, and the trained policy learns to be invariant to them, we expect that the policy will transfer well. More formally, we let  $\phi$  denote the parameters of an environment. The parameters encapsulate all the factors of variation between domains. Let  $P_{DR}(\phi)$  denote the distribution of domain parameters under domain randomization, and let  $\phi_{real}$  denote the parameters of the real world. The hypothesis underlying domain randomization is that  $P_{DR}(\phi_{real}) > 0$ , that is, the real world is in the support of the domain randomization distribution.<sup>1</sup>

Various DR variations have been explored in the literature, such as manipulating textures, lighting, camera position, and

<sup>1</sup>This definition assumes discrete distributions. For continuous distributions, a similar condition is: there is some area  $\phi_{real}$  where the performance of any policy does not change much, and  $\int_{\phi_{real}} P_{DR}(\phi) d\phi > 0$ .

---

**Algorithm 1** Validate on Sim, Detect on Real Score

---

**Require:** Policies  $\pi_1, \dots, \pi_k$ , trained using different DR parameters  $P_{DR_1}(\phi), \dots, P_{DR_k}(\phi)$ , single set of DR parameters for validation  $P_{DR_v}(\phi)$ , real world observations dataset  $\mathcal{D}_R$

- 1: **for**  $i = 1, \dots, k$  **do**
- 2:   Run  $\pi_i$  in sim  $P_{DR_v}(\phi)$  to get prior eval score  $p_i$
- 3:   Run  $\pi_i$  in sim  $P_{DR_i}(\phi)$  to get feature activations  $\mathcal{A}_S$
- 4:   Fit a two-component GMM  $G_i$  to  $\mathcal{A}_S$
- 5:   Feed-forward  $\mathcal{D}_R$  on  $\pi_i$  to get feature activations  $\mathcal{A}_R$
- 6:   Use  $G_i$  with  $\mathcal{A}_R$  to get OOD score  $l_i$
- 7:   Min-max normalize  $p_i', l_i' \leftarrow p_i, l_i$
- 8:    $VSDR_i \leftarrow p_i' \cdot l_i'$
- 9: **end for**
- 10: **return**  $VSDR_1, \dots, VSDR_k$

---

physical properties. In general, however, which DR setting works best for a given domain is not known in advance, and an iterative design process is followed, where the DR variation is tweaked based on the real world performance.

Following [31], during training, a new domain is randomized every one or more simulation steps. We term this the *frequency* of DR, and it is another hyperparameter that can be tweaked.

### C. Out of Distribution Detection

In this work, we build on the OOD approach of [24], which exploits the data used for training a network on some task, to detect whether a test sample is in distribution or not. Given  $M$  observations from the training domains  $o_1, \dots, o_M$ , we use them as input to the trained policy network, and collect the corresponding feature activations  $x_1, \dots, x_M$ . We then fit a parametric model  $P_\theta(x)$  to the features of the training data  $x_1, \dots, x_M$ , using maximum likelihood. Finally, we use the parametric model as a score of how much a test input  $o_{real}$  fits the observed data, by first extracting its features  $x_{real}$ , and then calculating the score  $l = \log P_\theta(x_{real})$ . Intuitively, for test inputs that are very different from the data, we expect the model to give a low likelihood, and therefore a low score.

Choosing which features of the network to include in the model, and which parametric model to fit, largely depends on the task and the data. [24] considered convolutional neural networks (CNNs), and in each layer, summed the activations that correspond to a particular channel, resulting in an activation that has the dimensionality of the number of channels in the layer. They fit a different Gaussian model for each layer, and used a weighted average of the models for the final score, where their weights were fit using labeled OOD examples.

## IV. METHOD

We now present our method for ranking policies based on combining validation in simulation and OOD detection in the real world. The method is summarized in Algorithm 1.

### A. Validation in Simulation

Following the DR hypothesis – that the real world can be seen as just another DR environment, a sufficient condition for a policy trained in simulation to perform well in the real world is that it performs well on every simulated domain within the support of  $P_{DR}$ . This can be measured by evaluating the policy on domains that were held out during training.

Formally, the training dataset for policy  $\pi_i$  contains  $N_{train}$  training domains  $\phi_1, \dots, \phi_{N_{train}}$ , sampled i.i.d. from  $P_{DR_i}$ . We also collect another set of  $N_{val}$  validation domains, sampled i.i.d. from  $P_{DR_v}$ , which is used to evaluate all policies. During training, the frequency in simulation steps in which a new domain  $\phi_i$  is drawn is a hyper-parameter. However, in validation we only draw a new domain  $\phi_k$  at the start of an episode and fix it for the remainder of the episode, similarly to how the real world domain is not changing during an episode.

Based on the simulated evaluation score we get our prior ranking, in which models are ranked according to the evaluated performance metrics (defined in V-A) in simulation under the above terms.

### B. OOD Detection in Real World

The second component in VSDR evaluates how likely are observations from the real-world, with respect to the observations seen during training. Thus, this part builds on two techniques: (1) real world data collection, and (2) OOD detection. We first explain (2), and then discuss (1) in detail.

As mentioned earlier, we are inspired by [24], and follow a similar OOD approach. We fit a two-component Gaussian Mixture Model to a dataset of layer embeddings collected in simulation, by running each of the tested policies in the exact same setting it was trained on, and running the observations through the policy network. In contrast to [24], which combined models of several layers into a single weighted score based on labeled OOD examples, in our work, we do not have such labeled outliers (we do not know in advance which real-world examples will be OOD for each policy). Therefore, we consider only single layers, and evaluate each one separately. In our experiments, we verify that our results hold for different choices of layers.

We next discuss how to obtain real-world observations for evaluating the OOD score. Ideally, the observations should correspond to states that are relevant to the task, and are also visited by the policy in simulation (so that we measure OOD in the visual domain only). In our work, we consider 3 data collection protocols:

- 1) **Expert**: Full demonstrations of an expert solving the task.
- 2) **Sparse-expert**: A sparse set of observations subsampled from the expert dataset above.
- 3) **Initial**: Only initial episode observations, randomly sampled from  $P_{init}$ .

All of the protocols are independent of the RL training method, and can be collected once and used for any trained

policy. Obviously, protocol (3) is easiest to generate, but for many tasks, teleoperation or scripted policies can be used to collect data for (1) and (2). We expect (1) to cover states that are relevant for the task, while not necessarily visited by the policy during training, and all the states in (3) to be visited by the policy, while possibly not covering all the important states in a successful trajectory. Protocol (2) is used to evaluate whether a complete trajectory is essential to our method or not. Finally, to evaluate the OOD score for a policy, denoted by  $l$ , we average its OOD score over all the observations in the real world dataset.

### C. Merging the Validation and OOD Scores

So far we described how to produce two scores for a policy – based on validation on sim, and OOD detection on real. We next describe how to combine the two scores into a single score.

The min-max normalization of a vector is defined as:

$$v_i' = \frac{\sum_i v_i - \min_i v_i}{\max_i v_i - \min_i v_i}$$

Normalizing and then multiplying together both the validation score  $p_i$  and the GMM’s log-likelihood score  $l_i$ , for a policy  $i$ , we get our VSDR score  $C_i$ ,

$$C_i = p_i' \cdot l_i'.$$

The motivation for multiplying the normalized scores is that we want a good policy to excel *in both* measures.

## V. RESULTS

In this section, we evaluate our model selection approach. We focus on answering the following questions:

- 1) Does the combined VSDR score improve upon using either score (validation on sim and OOD detection on real) separately?
- 2) How does VSDR compare to baselines?
- 3) How sensitive is our approach to different hyper-parameters selection?

Obviously, items (1) and (2) depend on the task, the RL algorithm, the number of trained models, the DR parameters, and the OOD method. To draw general conclusions, we opted to focus on a single, and rather generic, vision-based robotic grasping task, but performed an extensive evaluation of the different RL and DR parameters, trained models, and OOD method. While our results are expected to vary significantly between the different parameter settings, we shall see that general observations about the method can still be drawn.

### A. Evaluated Task - Grasping

We evaluate our method on a grasping task, based on the Lift task in Robosuite [32]. The task goal is to grasp a 4 cm wide cube located on a table in front of the robot, lift it to a height of at least 4 cm and hold it at that height. Each grasping attempt is limited to  $N_{steps}$  steps. For each grasping attempt, we calculate three performance metrics: Reward, Success and Strict-Success. Reward is the cumulative reward, taking into account both the reaching

and grasping stages of the task. An attempt is deemed a Success if on at least one step the goal criteria was met. An attempt is deemed a Strict-Success if the goal criteria was met in some step  $n_{succ}$ , and continues to be met for all steps  $n$  where  $n_{succ} < n \leq N_{steps}$ . In our experiments, in training and evaluation, in both simulation and real-world, we set  $N_{steps} = 20$ .

### B. Experimental Setup

We use a 7DoF Franka Panda robotic arm in both simulation and the real-world, with a 4D Cartesian position-based impedance controller.

**Input:** The camera observations are retrieved from a fixed RGB camera (Intel RealSense D415) positioned in front of the robot looking downwards at the table. The image is downsampled to 267x267 resolution and is then center cropped during evaluation, or randomly cropped during training into a 224x224 image, as suggested in RAD [28]. An image of the real-world setup can be seen in Figure 1. The observation also includes a proprioceptive component, comprised of the sines and cosines of the joint angles, 3D end-effector Cartesian position and orientation (4D quaternion), and gripper finger positions. **Output:** Actions consist of the requested changes in 3D Cartesian position and in rotation of the gripper along the vertical axis, and a binary gripper open/close command. **Network Architecture:** We have used an SAC [27] agent, with neural network architecture similar to the one described in [33] to solve the task in simulation. Unlike [33], we used a ResNet18 [34] encoder to process a 224x224 image. As in [33], the image encoder is followed by actor and critic networks, both of which are 3-layer MLPs with ReLU activations following each layer except the last. **Simulation:** We use the Robosuite simulation framework [32]. We first sample two sets of domain datasets to be used during training and prior evaluation. All our models are trained on domains from the training domains dataset, but are then evaluated on the validation domains dataset in order to get the validation score  $p$ . **Real World:** We fixed the lab lighting by shading the windows and using only artificial light for a fair comparison between all our tested models. To control the robot we use ROS [35] with Franka Panda libraries from [36]. To facilitate automated testing, we implemented a heuristic pick-and-place policy for placing the cube at desired positions. **Baselines:** We compare VSDR to the SoftOPC and OPC metrics [14]. **Model Categories:** We trained policies using a variety of DR configurations, which we divide into the following categories:

- **DR-heavy-freq-n:** For each object in the scene: Randomize the textures (programmatically generated by the simulator) and material properties. For each lighting source: Randomize activation, position, direction and diffuse, ambient and specular properties. For each camera: Randomize position, angle and field-of-view. **freq-n** refers to the simulation steps frequency in which a new domain is applied, where  $n \in \{0, 1, 2, 5\}$ .  $n = 0$  stands for randomizing a new domain once per episode at reset.

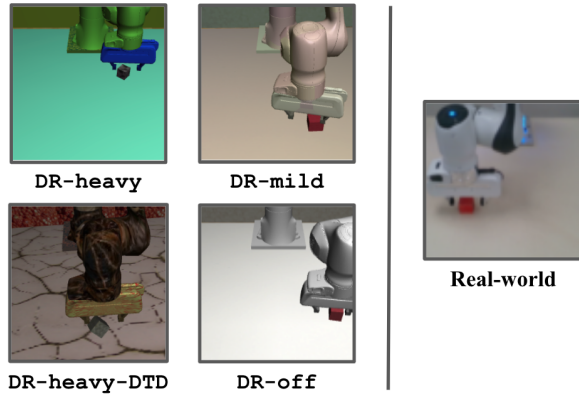


Fig. 2: Examples of image observations from simulation (2 left columns) and real-world (rightmost column).

- **DR-mild-freq-n**: Same as **DR-heavy-freq-n**, but the randomization is taken as a small perturbation around the original object texture and material.
- **DR-dtd**: Same as **DR-heavy-freq-1**, with object textures sampled **only** from the DTD Dataset (no programmatically generated textures).
- **DR-heavy-dtd**: Same as **DR-heavy-freq-1**, with both programmatically generated textures and textures from DTD. The texture has a 20% chance of being sampled from DTD.
- **DR-heavy-lights-always-on**: Same as **DR-heavy-freq-1**, only that the lights are never turned off.
- **DR-heavy-light-params-sweep**: Same as **DR-heavy-freq-1**, with stronger randomization of the diffuse, ambient and specular properties of each light source. We increase the randomization for each property separately and for all combinations, for a total of 8 models.
- **DR-off**: No randomization is applied.

Combining all of the above, we have a 20 distinct model types. For each model type we trained 3 seeds, for a total of 60 models overall. Some example image observations are shown in Figure 2.

### C. Experiments

To measure the goodness of a model selection method, we compute the Spearman rank correlation coefficient  $\rho$  [37] between the ranking produced by the method and the ground-truth (GT) ranking. The GT ranking is the ranking of models by their real-world performance. To evaluate real-world performance, each model was tested on 49 grasp attempts (a 7x7 grid of initial cube positions). We generated 3 GT rankings, based on the *Reward*, *Success*, and *Strict-Success* metrics defined in section V-A. Average real-world *Success* rate was 30% across models, ranging from 0% to 92%. To evaluate what factor of our results is attributed to noise in the real-world setting, we performed 2 independent evaluation cycles in the real-world (a total of approx. 130 robot hours) and calculated the Spearman

TABLE I: Real-world run-to-run correlation, based on the metrics defined in Section V-A

	Run 1 Mean	Run 2 Mean	Spearman $\rho$
Reward	15.49	15.39	0.98
Success	32.0%	30.1%	0.97
Strict-Success	17.6%	16.9%	0.93

$\rho$  between them – this is an upper bound for any ranking method. Details are provided in Table I.

We experiment with 3 types of validation in simulation, using the following DR configurations: **DR-heavy-freq-0**, **DR-mild-freq-0** and **DR-off**. For the first two, the domains come from the validation domains dataset we collected in advance. Each prior score was computed based on 2,000 episodes.

For the GMM fitting, we consider features from by five different layers in the model network – the output of the ResNet18 image encoder, referred to as *img\_encoder* and the first four layers in the actor MLP, referred to as *fc0*, *relu0*, *fc1* and *relu1*.

For evaluating the real-world OOD scores, we collected a dataset of expert demonstrations, consisting of 64 grasp trajectories (grid of 8x8 initial cube positions), executed by a scripted policy. The total number of observations in this dataset is 704. We apply the data collection protocols defined in section IV-B to the expert dataset: For *Expert* we use the entire dataset. For *Sparse-expert* we uniformly sample 100 observations from the dataset. For *Initial* we take the initial step from each trajectory in the dataset, for a total of 64 observations.

To calculate the OPC/SoftOPC baselines, full trajectories are required, both successful and failing. [14] used 4000 real-world trajectories, generated by two policies with a success rate of approx. 40%. To be able to calculate OPC/SoftOPC with a dataset of size of similar order, we used all the real-world trajectories we collected during GT evaluation of all trained policies, for a total of 2940 episodes (approx. 53k transitions), with a success rate of approx. 30%. Note that this gives a very strong advantage to the baseline, which effectively trains on ground truth data! Nevertheless, our results show that VSDR, which only has access to real-world data that does not depend on the trained policies, is able to outperform OPC/SoftOPC on our evaluated task.

1) *Main Results and Analysis*: Figure 3 shows the Spearman rank correlations for our method and the baselines, for all combinations of fitted GMMs, sim validation types, and performance metrics. We note that the combined VSDR score outperforms the separate component scores in mostly all combinations. We also observe that VSDR consistently outperforms the OPC/SoftOPC baselines, despite the disparity in amount of data shown to each method. In addition, we see that combining the sim validation score with OPC/SoftOPC improves these metrics as well, although VSDR still produces the best correlation in most cases. This shows that the idea of combining validation in sim with performance

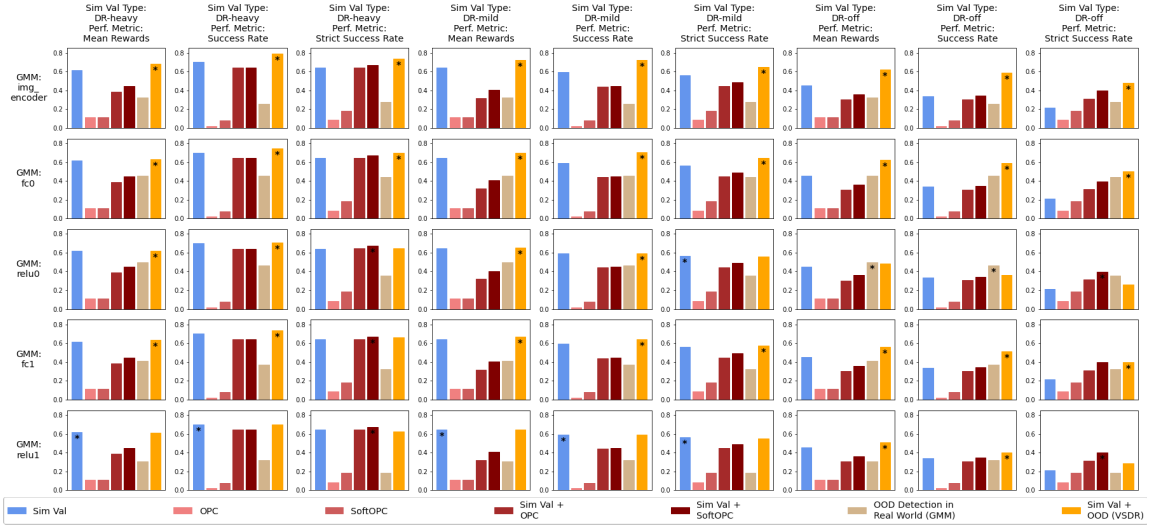


Fig. 3: Spearman rank correlations between rankings produced by different model selection methods and the GT ranking. All 60 models are ranked. Each column refers to a specific combination of simulation validation type and performance metric. Note that each performance metric implies a different GT ranking. Each row of plots refers to the layer based on which the GMM was fitted. The best correlation within each plot is denoted by \*.

in real generalizes beyond our OOD method. Note however, that in these results OPC/SoftOPC still use GT data, and therefore these combined methods are not practical for our model selection desiderata.

The results in Figure 3 were obtained using the *Sparse-expert* data collection protocol, that is - with 100 real-world observations. Results using *Expert* (704 observations) and *Initial* (64 observations) were similar, as shown in Figure 4. This highlights the small amount of data sufficient for our method, and also shows that complete trajectories are not a requirement. In addition, we observed that sub-sampling different sets of observations as part of the *Sparse-expert* protocol did not have significant impact on the results. In our experiments, the standard deviation for the correlations based on the VSDR score obtained from different sub-sampled sets, ranged between 0.0004 to 0.02. Collectively, these results display the robustness of our approach to different hyper-parameters.

2) *Models Separability*: We show how correlation with the GT improves when the set of models is more separable. Two approaches for making the models more separable are: (1) Having fewer seeds per model type; (2) Removing very similar model types. In Figure 5 we show results for both approaches – first we remove seeds, and then we remove 5 out of the 8 DR-heavy-light-params-sweep models, keeping only the DR types where a single lighting property was changed.

## VI. CONCLUSIONS

We proposed a method for choosing the best models to deploy in the real-world that are likely to best cross the sim-to-real gap. Our method requires merely dozens real-world observations in order to evaluate how novel is the real world domain comparing to the domains each policy has

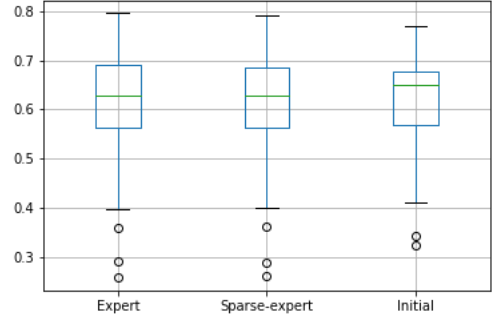


Fig. 4: Box plots of Spearman correlations of VSDR based rankings with GT rankings, for all 60 models, for all data collection protocols defined in section IV-B. For each protocol, the plot is based on the correlations for all combinations of sim validation types, performance metrics and layer for fitting the GMM.

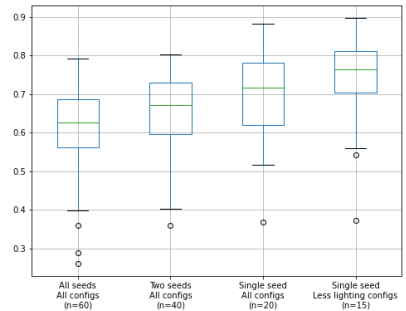


Fig. 5: Box plots of Spearman correlations of VSDR based rankings with GT rankings, across different sets of models. The leftmost plot is based on the full 60 models set. Each plot going in the right direction is based on a smaller, more separable set of models. We observe that the correlation improves as the set of models becomes more separable.



observed during simulation, and outperforms baselines from the literature. In this work we focused on image observations, and DR methods that modify the visual appearance of the scene. It is interesting to extend this approach to domains where physical properties such as mass and friction are varied using DR as well.

## APPENDIX

Additional details and implementation will be available [here](#).

## ACKNOWLEDGMENT

Aviv Tamar is partly funded by the the Open Philanthropy Project Fund – an advised fund of Silicon Valley Community Foundation, and a grant from Intel Corporation.

## REFERENCES

- [1] J. Kober, J. A. Bagnell, and J. Peters, “Reinforcement learning in robotics: A survey,” *The International Journal of Robotics Research*, vol. 32, no. 11, pp. 1238–1274, 2013.
- [2] F. Golemo, A. A. Taiga, A. Courville, and P.-Y. Oudeyer, “Sim-to-real transfer with neural-augmented robot simulation,” in *Proceedings of The 2nd Conference on Robot Learning*, vol. 87. PMLR, 29–31 Oct 2018, pp. 817–828.
- [3] J. Tan, T. Zhang, E. Coumans, A. Iscen, Y. Bai, D. Hafner, S. Bohez, and V. Vanhoucke, “Sim-to-real: Learning agile locomotion for quadruped robots,” *Robotics: Science and Systems XIV*, Jun 2018.
- [4] X. B. Peng, M. Andrychowicz, W. Zaremba, and P. Abbeel, “Sim-to-real transfer of robotic control with dynamics randomization,” in *2018 IEEE International Conference on Robotics and Automation (ICRA)*, May 2018, pp. 3803–3810.
- [5] J. Hwangbo, J. Lee, A. Dosovitskiy, D. Bellicoso, V. Tsounis, V. Koltun, and M. Hutter, “Learning agile and dynamic motor skills for legged robots,” *Science Robotics*, vol. 4, no. 26, p. eaau5872, Jan 2019.
- [6] OpenAI, M. Andrychowicz, B. Baker, M. Chociej, R. Józefowicz, B. McGrew, J. Pachocki, A. Petron, M. Plappert, G. Powell, A. Ray, and et al., “Learning dexterous in-hand manipulation,” *The International Journal of Robotics Research*, vol. 39, no. 1, p. 3–20, Nov 2019.
- [7] OpenAI, I. Akkaya, M. Andrychowicz, M. Chociej, M. Litwin, B. McGrew, A. Petron, A. Paino, M. Plappert, G. Powell, R. Ribas, J. Schneider, N. A. Tezak, J. Tworek, P. Welinder, L. Weng, Q. Yuan, W. Zaremba, and L. Zhang, “Solving rubik’s cube with a robot hand,” *arXiv preprint arXiv:1910.07113*, 2019.
- [8] S. James and E. Johns, “3d simulation for robot arm control with deep q-learning,” *arXiv preprint arXiv:1609.03759*, 2016.
- [9] S. James, P. Wohlhart, M. Kalakrishnan, D. Kalashnikov, A. Irpan, J. Ibarz, S. Levine, R. Hadsell, and K. Bousmalis, “Sim-to-real via sim-to-sim: Data-efficient robotic grasping via randomized-to-canonical adaptation networks,” in *Proceedings of the IEEE/CVF Conference on Computer Vision and Pattern Recognition*, 2019, pp. 12 627–12 637.
- [10] J. Tobin, R. Fong, A. Ray, J. Schneider, W. Zaremba, and P. Abbeel, “Domain randomization for transferring deep neural networks from simulation to the real world,” in *2017 IEEE/RSJ international conference on intelligent robots and systems (IROS)*. IEEE, 2017, pp. 23–30.
- [11] F. Sadeghi and S. Levine, “Cad2rl: Real single-image flight without a single real image,” in *Proceedings of Robotics: Science and Systems*, Cambridge, Massachusetts, July 2017.
- [12] P. Henderson, R. Islam, P. Bachman, J. Pineau, D. Precup, and D. Meger, “Deep reinforcement learning that matters,” in *Proceedings of the AAAI conference on artificial intelligence*, vol. 32, 2018.
- [13] T. Zahavy, Z. Xu, V. Veeriah, M. Hessel, J. Oh, H. van Hasselt, D. Silver, and S. Singh, “Self-tuning deep reinforcement learning,” *arXiv preprint arXiv:2002.12928*, 2020.
- [14] A. Irpan, K. Rao, K. Bousmalis, C. Harris, J. Ibarz, and S. Levine, “Off-policy evaluation via off-policy classification,” in *Advances in Neural Information Processing Systems*, vol. 32, 2019.
- [15] M. Dudik, J. Langford, and L. Li, “Doubly robust policy evaluation and learning,” in *Proceedings of the 28th International Conference on Machine Learning*, ser. ICML ’11. ACM, June 2011, pp. 1097–1104.
- [16] N. Jiang and L. Li, “Doubly robust off-policy value evaluation for reinforcement learning,” in *Proceedings of The 33rd International Conference on Machine Learning*, ser. Proceedings of Machine Learning Research, vol. 48. PMLR, 20–22 Jun 2016, pp. 652–661.
- [17] D. Precup, R. S. Sutton, and S. P. Singh, “Eligibility traces for off-policy policy evaluation,” in *Proceedings of the Seventeenth International Conference on Machine Learning*, ser. ICML ’00. San Francisco, CA, USA: Morgan Kaufmann Publishers Inc., 2000, p. 759–766.
- [18] P. Thomas, G. Theodorou, and M. Ghavamzadeh, “High-confidence off-policy evaluation,” in *Proceedings of the AAAI Conference on Artificial Intelligence*, vol. 29, no. 1, 2015.
- [19] T. L. Paine, C. Paduraru, A. Michi, C. Gulcehre, K. Zolna, A. Novikov, Z. Wang, and N. de Freitas, “Hyperparameter selection for offline reinforcement learning,” *arXiv preprint arXiv:2007.09055*, 2020.
- [20] B. Schölkopf, J. Platt, J. Shawe-Taylor, A. Smola, and R. Williamson, “Estimating support of a high-dimensional distribution,” *Neural Computation*, vol. 13, pp. 1443–1471, 07 2001.
- [21] D. M. J. Tax and R. P. W. Duin, “Support vector data description,” *Mach. Learn.*, vol. 54, no. 1, pp. 45–66, Jan. 2004.
- [22] S. Zhai, Y. Cheng, W. Lu, and Z. Zhang, “Deep structured energy based models for anomaly detection,” in *Proceedings of The 33rd International Conference on Machine Learning*, ser. Proceedings of Machine Learning Research, vol. 48. PMLR, 20–22 Jun 2016, pp. 1100–1109.
- [23] T. Schlegl, P. Seeböck, S. M. Waldstein, U. Schmidt-Erfurth, and G. Langs, “Unsupervised anomaly detection with generative adversarial networks to guide marker discovery,” in *International Conference on Information Processing in Medical Imaging*. Springer, 2017, pp. 146–157.
- [24] K. Lee, K. Lee, H. Lee, and J. Shin, “A simple unified framework for detecting out-of-distribution samples and adversarial attacks,” in *Advances in Neural Information Processing Systems*, vol. 31, 2018.
- [25] E. Zisselman and A. Tamar, “Deep residual flow for out of distribution detection,” in *Proceedings of the IEEE/CVF Conference on Computer Vision and Pattern Recognition*, 2020, pp. 13 994–14 003.
- [26] R. S. Sutton and A. G. Barto, *Reinforcement learning: An introduction*. MIT press, 2018.
- [27] T. Haarnoja, A. Zhou, P. Abbeel, and S. Levine, “Soft actor-critic: Off-policy maximum entropy deep reinforcement learning with a stochastic actor,” in *Proceedings of the 35th International Conference on Machine Learning*, ser. Proceedings of Machine Learning Research, vol. 80. PMLR, 10–15 Jul 2018, pp. 1861–1870.
- [28] M. Laskin, K. Lee, A. Stooke, L. Pinto, P. Abbeel, and A. Srinivas, “Reinforcement learning with augmented data,” in *Advances in Neural Information Processing Systems*, vol. 33, 2020, pp. 19 884–19 895.
- [29] J. Matas, S. James, and A. J. Davison, “Sim-to-real reinforcement learning for deformable object manipulation,” in *Proceedings of The 2nd Conference on Robot Learning*, ser. Proceedings of Machine Learning Research, vol. 87. PMLR, 29–31 Oct 2018, pp. 734–743.
- [30] F. Sadeghi, A. Toshev, E. Jang, and S. Levine, “Sim2real viewpoint invariant visual servoing by recurrent control,” in *Proceedings of the IEEE Conference on Computer Vision and Pattern Recognition (CVPR)*, June 2018.
- [31] T. Dai, K. Arulkumaran, T. Gerbert, S. Tukra, F. Behbahani, and A. A. Bharath, “Analysing deep reinforcement learning agents trained with domain randomisation,” *arXiv preprint arXiv:1912.08324*, 2019.
- [32] Y. Zhu, J. Wong, A. Mandlekar, and R. Martín-Martín, “robosuite: A modular simulation framework and benchmark for robot learning,” *arXiv preprint arXiv:2009.12293*, 2020.
- [33] D. Yarats, A. Zhang, I. Kostrikov, B. Amos, J. Pineau, and R. Fergus, “Improving sample efficiency in model-free reinforcement learning from images,” *arXiv preprint arXiv:1910.01741*, 2019.
- [34] K. He, X. Zhang, S. Ren, and J. Sun, “Deep residual learning for image recognition,” in *Proceedings of the IEEE Conference on Computer Vision and Pattern Recognition (CVPR)*, June 2016.
- [35] M. Quigley, B. Gerkey, K. Conley, J. Faust, T. Foote, J. Leibs, E. Berger, R. Wheeler, and A. Ng, “Ros: an open-source robot operating system,” in *ICRA Workshop on Open Source Robotics*, vol. 3, may 2009.
- [36] S. Sidhik. (2020) Franka ros interface: A ros/python api for controlling

and managing the franka emika panda robot (real and simulated).  
[Online]. Available: <https://doi.org/10.5281/zenodo.4320612>

- [37] C. Spearman, "The proof and measurement of association between two things," *The American Journal of Psychology*, vol. 15, no. 1, pp. 72–101, 1904. [Online]. Available: <http://www.jstor.org/stable/1412159>